1955

Deflection stability (shakedown) of continuous-frames, Dec. 1955, Interim Report No. 28

A. T. Gozum

G. Haaijer

Lehigh University

INSTITUTE OF RESEARCH

Welded Continuous Frames and Their Components

INTERIM REPORT No. 28

DEFLECTION STABILITY ("SHAKEDOWN") OF CONTINUOUS BEAMS

by

ALFREDO T. GOZUM and GEERHARD HAAIJER

(Not for Publication)

WELDED CONTINUOUS FRAMES AND THEIR COMPONENTS

Interim Report No. 28

DEFLECTION STABILITY ("SHAKEDOWN) OF CONTINUOUS BEAMS

by

Alfredo T. Gozum and Geerhard Haaijer

Fritz Engineering Laboratory
Department of Civil Engineering
Lehigh University
Bethlehem, Penna.

December, 1955

Fritz Laboratory Report 205G.1

TABLE OF CONTENTS

I. INTRODUCTION

The plastic strength ("collapse" load) of statically indeterminate structures is usually determined, theoretically and experimentally, through the application of a system of proportional steadily increasing loads. However, when the loads are varied within certain limits, either independently of each other or in a certain loading pattern, the structure may continue to deform plastically upon repeated application of the loads. This type of failure has been discussed for example by Symonds[1]* . The problem is to determine critical limits such that, if not exceeded by the variable loads, plastic deformation will cease after some repeated application of the loads, due to a state of residual stress caused by the initial plastic deformation. Then the deflections of the structure will stabilize with a cessation of further progressive deformations. The term "shakedown" has been used to describe this process. Consequently, the set of critical limits is called the stabilizing (or "shakedown") load. It is felt that the term "stabilizing load" used in this report is more descriptive of the actual phenomenon than "shakedown load".

Massonnet[2] carried out tests on a structure with loads applied and removed in a random manner but encountered difficulties due to lateral buckling. Neal[3] summarized the work of previous investigators on the shakedown theory of

- -

* See list of references

trusses. He also investigated corresponding phenomena of continuous beams and plane frames[4] and stated:

> "If any state of residual stress can be found for a structure that enables all further variations of the external loads between their prescribed limits to be supported in a purely elastic manner, then the structure will skakedown".

The object of the tests described in this report was to investigate experimentally the behavior of a statically indeterminate structure under the application of proportional loads and of repeated variable loads. The selected structure was a continuous beam, simply supported over two equal spans and carrying two concentrated loads at points symmetrical about the central support (Figure 1). Furthermore, a theoretical analysis of the structure is presented as a basis for the comparison of experimental results with theoretical predictions.

II. THEORETICAL ANALYSIS

1. Proportional Loading

The structure, a two-span continuous beam, is shown in Fig. 1. The points of support and load application are numbered 1, 2, 3, 4 and 5. It is commonly assumed that all plastic deformation takes place in plastic hinges which, when the ultimate load is reached, are developed in sufficient number to make the structure a mechanism. With this simplifying assumption maximum loads and load-deflection relations can be

derived in a simple manner[6]. Possible locations of plastic hinges are 2, 3, and 4, the points of extreme bending moment.

Two loading conditions are considered:

(a) Symmetric loading by two equal loads (Fig. 1).

(b) Single load applied to one span only (Fig. 2).

Figures 1 and 2 also show the mechanisms formed at the computed ultimate load, the plastic hinges being indicated by circles. The ultimate load, P_u, is the same for both cases.

$$P_u = 20\ M_p/3L \quad . \quad . \quad . \quad . \quad . \quad . \quad (1)$$

with M_p = full plastic moment of the section. It is interesting to note that although the maximum loads are equal for cases (a) and (b), the sequence of formation of the plastic hinges is reversed. Consequently, the load vs. deflection curves differ as shown in Fig. 3[6].

2. Cyclic Loading

The structure being symmetrical, only deformations of sections 2 and 3 will be analyzed. When the structure is subjected to independently varying loads beyond certain critical limits to be defined later (none of which would produce simultaneous formation of plastic hinges) rotations (in the same sense) can be built up at these sections. If loads as shown in Figures 1 and 2 compose the loading cycle, in case (a) Hinge 3 is rotated while in case (b) this occurs at Hinge 2. As a result, the deflection at Point 2 is increased at the end of each cycle. Such cyclic repetitions will eventually produce excessive deflections.

The continued deflection as each cycle is applied can only occur in a statically indeterminate structure wherein residual moments exist as a consequence of plastic deformation. An example of this occurs in case (a), Figure 1, when the beam is loaded as shown and Section 3 deforms plastically. The equal loads are subsequently removed and under this zero load condition, the plastic deformation of Section 3 would deflect point 1 downward were the support at this point removed. Hence there exist positive residual moments in the beam with the zero loads. A single load as in case (b) is applied next and when the sum of the positive residual moment and the super-imposed bending moment at Section 2 equals the plastic moment of the section, the deflection will increase a finite amount. Section 2 may behave in similar fashion for the loading sequence case (b) to case (a) causing an increase of the deflections.

After sufficient applications of the cyclic loads, the structure may have acquired a particular set of residual moments whereby all further applications of the loads up to a prescribed limit will be supported in an elastic manner. This prescribed limit is the stabilizing ("shakedown") load above which deflections will continue to increase, resulting in excessive deformations of the structure.

Due to conditions inherent in the chosen test set-up, a single concentrated load necessary for maximum bending moment at Section 2 could not be realized but was accompanied by a one-kip load acting on the adjacent span as shown in Figure 4(b).

In the following theoretical derivations this minimum value of P has been chosen ξP, ξ being a numerical coefficient less than unity. Maximum moment for Section 3 occurred for the loading condition shown in Figure 4(a). The elastic bending moment diagrams for both loading conditions are shown in Figures 4(a) and 4(b). The residual moment diagram can only have the shape shown in Figure 4(c). The necessary condition of the "shakedown" theory that the sum of the residual moment and the superimposed bending moment must not exceed the plastic moment of the section leads to the following inequalities for sections 2 and 3 respectively:

$$\frac{PL}{625}(114 - 36\xi) + \frac{3}{5}M_r \leq M_p \quad . \quad . \quad . \quad (2)$$

$$-\frac{120}{625}PL + M_r \geq -M_p \quad . \quad . \quad . \quad . \quad . \quad (3)$$

with

M_r = residual moment at 3

In the limiting case the equal signs are valid. Solving equations (2) and (3) then gives the critical stabilizing load, P_s.

$$P_s = \frac{1000}{186-36\xi}\left(\frac{M_p}{L}\right) \quad . \quad . \quad . \quad . \quad . \quad (4)$$

When the structure is loaded at Point 4 only, the moment at 2 reverses and could cause plastic rotation in the opposite direction. This phenomena is called alternating plastic flow, which also must be avoided in order to obtain completely elastic

behavior. Calling ΔM_y the total available elastic moment range, this condition can be expressed by the following inequality

$$\frac{P_s L}{625}(114 - 36\zeta) + \frac{P_s L}{625}(36 - 114\zeta) \leq \Delta M_y \quad .. \quad (5)$$

Simplifying inequality (5):

$$P_s \leq \frac{25}{6(1-\zeta)}\left(\frac{\Delta M_y}{L}\right) \quad . \quad . \quad . \quad . \quad . \quad . \quad (5a)$$

Equations (4) and (5a) each determine a value of P_s. Obviously the lowest of the two is the actual stabilizing load.

3. The Influence of Strain-Hardening

The above theoretical derivations are based on the simplifying assumption that the maximum moment a section can sustain is its full plastic moment, M_p. However, due to strain-hardening of the material moments larger than M_p can be carried[8]. When a beam is subjected to a constant moment the influence of strain-hardening will start when the angle of rotation per unit length has reached the value ϕ_{st} corresponding to a strain of the outer fiber ε_{st}. As the ratio of the strain at strain-hardening, ε_{st}, to the strain at which yielding starts, ε_y, is of the order of 10 to 15 the influence will only become apparent after relatively large deformations. When the beam is subjected to a moment gradient the influence is felt immediately after yielding has started. This is the case for the loading conditions of Fig. 1 and Fig. 2. Therefore the actual behavior can be expected to be quite different from the simplified load deflection curves shown in Fig. 3.

Consider first loading condition (a) with two equal loads which are steadily increased but kept equal (proportional loading). For certain values of the loads, P_p, the moment at sections 2 and 3 will have values M_2 and M_3 respectively and the deflection at the loading points will have a certain value δ_s. The loads, P_p, can be expressed in terms of M_2 and M_3 as follows:

$$P_p = \frac{1}{L}\left(\frac{25}{6} M_2 - \frac{5}{2} M_3\right) \quad . \quad . \quad . \quad . \quad . \quad . \quad (6)$$

Assume next that the loads are varied between the limits ζP_L and P_L in such a manner that symmetrical deformations are produced as in the above considered case of proportional loading. Then the deformations will stabilize at the same value, δ_s, of the deflections of the loading points if the following equations are satisfied:

$$\frac{P_L L}{625}(114 - 36\zeta) + \frac{3}{5} M_r = M_2 \quad . \quad . \quad . \quad . \quad (7)$$

$$-\frac{120}{625} P_L L + M_r = M_3 \quad . \quad . \quad . \quad . \quad . \quad . \quad (8)$$

Solving equations (7) and (8) gives

$$P_L = \frac{625}{186-36\zeta} \frac{M_2 - 3/5\, M_3}{L} \quad . \quad . \quad . \quad . \quad (9)$$

Comparing equations (6) and (9) shows that

$$\frac{P_L}{P_p} = \frac{150}{186-36\zeta} \quad . \quad . \quad . \quad . \quad . \quad . \quad . \quad (10)$$

The same reasoning could be applied to case b with proportional loading and with cyclic loading producing the same deformations. The result would be identical with equation (10).

The important conclusion is that the same deflections which occur under proportional loading up to load P_p can be obtained if the loads are varied between the limits $\pm P_L$ and P_L. The ratio of P_L and P_p is then given by equation (10).

III. EXPERIMENTAL INVESTIGATION

1. Test Set-Up

The test set-up is shown in Figures 5, 6 and 7. Instead of the downward acting concentrated loads at points 2 and 4 (Fig. 1) forces were applied in the upward direction by hydraulic jacks. In this way the jacks and the supports were acting in tension and a simple set-up was obtained by attaching them to a rigid frame surrounding the specimen.

To simulate simple supports, thin plates were welded to the specimen, the moment of inertia of the central support being approximately 1/250 of that of the specimen.

The loads applied by the jacks were measured by dynamometers. Furthermore, SR-4 gages were attached at both end supports in order to measure the end reactions.

Analysis shows that the ratio of the maximum load under proportional loading and the stabilizing load of the structure increases when the points of load application approach the central support. In order to be able to determine this ratio experimentally it was desired that the theoretical ratio of ultimate to stabilizing load be not less than 120%. On the other hand the moment gradient should not be too steep to minimize the effect of shearing forces. Accordingly, the load points were chosen at a distance of 2/5 of the span length from the central support.

The specimens were cut from an as-delivered 4WF13 rolled beam, taken from the middle third of a rolling. A span length of 4 feet was considered sufficient for this program. Since tests were to be carried out far into the plastic range, lateral buckling was avoided by testing the specimens, about their weak axis. The loading and support stiffeners were welded to the specimens prior to stress relieving treatment. Thus all specimens were practically free of any residual stresses due to cold bending and welding. The beams were whitewashed in order to make a qualitative study of the yielding process. The plate supports were also whitewashed such that possible yield lines due to stress concentration could be observed.

Deflections and rotations were measured with Ames dials, the deflection measurements being taken at the load points and the supports and the rotation measurements being

taken at the plastic hinges (Sections 2, 3 and 4). The rotation indicators were installed to measure the relative rotation of two cross-sections separated by a distance equal to the depth of the beam.

Finally, the loading jacks were carefully aligned with the axis of the specimen to assure equal distribution of the loads to both flanges.

2. Test Program

The tests are summarized in Table 1. First two tests, P-1 and P-2, were performed with proportional, steadily increasing loads to investigate the actual behavior under the loading conditions of case (a) and (b) (Figs. 1 and 2). As the jack-beam connections and the supports were designed to act in tension, zero loads were replaced by a minimum load of one kip. In the plastic range readings were taken after loads and deflections had stabilized.

In test P-1 the residual moments were measured. This was done by removing the loads after applying the load of 17.7 kips. The residual moments could then be determined from the measured end reactions.

Cyclic loading tests were performed next on three specimens, C1, C2 and C3. Table 1 shows the steps constituting one cycle, P_L being the upper limit of a chosen load range. The procedure followed for starting the cyclic test was to bring both equal loads to the chosen upper limit corresponding

to Step (a) with readings taken at appropriate increments. Thereafter, readings were taken after each step was completed. Step (e) concluded one cycle. Consequently, the deformations at Step (e) were taken as a basis of comparison for determining the progress of deformation with increasing number of cycles.

A sufficient number of loading cycles was applied until deformations stabilized. Test C-1 was carried out with a relatively large value of the upper limit, P_L. With tests C-2 and C-3, P_L was increased each time the deformations stabilized.

Four representative tension coupons were tested in a 60,000 lb. hydraulic machine with a valve opening corresponding to a strain rate of 1 micro in./in. per sec. Loads and strains were recorded with a Templin automatic stress-strain recorder using a gage length of 8 in. The tension coupons were dimensioned according to A.S.T.M. standards. The geometrical properties of the section were determined with micrometers; the measurements were checked against carbon imprints.

3. Test Results

A summary of properties of the 4WF13 shape tested in this program is shown in Table 2. Also included are the section properties derived from the material and geometrical properties. With these section properties, values of critical loads predicted by theory can now be derived.

The predicted maximum load under proportional loading is given by equation (1)

$$P_u = 16.81 \text{ kips}$$

Values of the stabilizing load are obtained from equation (4):

$$P_s = 13.72 \text{ kips}$$

and from equation 5a:

$$P_s \leq 14.85 \text{ kips}$$

Thus, being the smallest of the two, the first value is the theoretical critical stabilizing load.

In Fig. 8 the load vs. deflection curve is plotted for the proportional loading test P-1. The deflection values plotted are the mean values of the deflections at the two load points. Most previous tests have given an obvious maximum value of the load. However, in this case no such convenient "leveling off" point was observed because of the point loading and elimination of buckling. Fig. 9 shows the load vs. deflection curve for test P-2.

In Figs. 8 and 9 the value at the intersection of the elastic and plastic slope lines has been selected as the experimental ultimate load. At this load the deflection starts to increase "more rapidly" and therefore this criterion is called a deflection-rate criterion. The experimental values

obtained are:

Case (a) (Test P-1) P_u = 17.08 kips (101.5% of its theoretical value)

Case (b) (Test P-2) P_u = 17.68 kips (105% of its theoretical value)

Massonnet[2] defined as "experimental collapse load" the load at which the deflection is twice the deflection at the intersection of elastic and plastic slope lines (deflection criterion). For Cases (a) and (b) this results in P_u = 17.58 kips and P_u = 17.78 kips respectively.

From the observed values of the end reactions, the moments at sections 2 and 3 were computed and plotted vs. the applied load in Figure 10 for test P-1 and in Fig. 11 for test P-2. Theoretically, when both moments at these two points attain the full plastic moment of the section, the structure reaches its maximum load. As shown in Figure 11, the moments M_2 and M_3 became nearly equal in magnitude at a load of 16.0 kips. In test P-2 (Fig. 11) M_2 and M_3 came close to each other at a load of 18.0 kips. The full plastic moment of the section based on the average lower yield stress of the tension coupons (Table 1) was 121.0 in-kips. Both figures also show good agreement of observed values with theoretical predictions within the elastic range.

During test P-2 the structure was completely unloaded after being loaded to 17.7 kips. Fig. 10 shows the existence of residual moments.

As mentioned previously, rotation measurements were taken using a gage length equal to the depth of the beam. The mean values of the moment over the gage length, M', have been computed in addition to the extreme values at the loading points and center support. Figs. 12 and 13 show the experimental and idealized M-Ø curves for both proportional loading tests, Ø being the rotation per unit length (curvature). The idealized curve was derived from the geometrical and material properties of the section neglecting the influence of strain-hardening. The test results indicate again that the cross-section is capable of developing a greater resistance than the plastic moment.

Results of the three cyclic loading tests, C-1, C-2 and C-3, are shown in Fig. 14 with the number of cycles plotted vs. the average deflections at the end of step (e) of the cycle (Table 1). Test C-1 represents a case of typical progressive deformation. The test was stopped when the deflections reached 1.2 inches. Although the deflections had not yet stabilized, it appears from Fig. 14 that stabilization would have occurred at a deflection of perhaps 1.3 to 1.4 in. Test C-2 was started with an upper limit of 14.75 kips and stabilized fairly well after 6 cycles. Subsequent increments of 250 lbs. were next applied up to a limit of 15.25 kips. For all these loads the deformations stabilized after 6 cycles. At 16.0 kips stabilization had not yet occurred after 6 cycles, though it would have with more repetitiousness. Finally, Test C-3 was performed to check the results of Test C-2. Eventually it stabilized.

In Fig. 15 the load deflection curve for test P-1 has been replotted. From this curve a P_L vs. δ_s curve has been derived by the use of equation (10) and is compared with the test results in the same figure. Defining as the experimental critical stabilizing load the value of P_L at which the stabilized deflection, δ_s, starts to increase more rapidly, gives

P_s = 14.8 kips (108% of the theoretical stabilizing load)

The test results are summarized in Table 3.

Finally, the behavior of the beam under cyclic loading will be illustrated by analyzing steps (a), (b) and (c) of the first cycle of test C-1.

Shown in Fig. 17a are the observed moment diagrams of step (a) and the computed corresponding elastic moments. The difference between elastic and observed moments is cross-hatched in the figure. Complete unloading would occur in a purely elastic manner and positive residual moments, M_r, would be left in the structure (Figure 17b). Applying the load of step (d) as shown in Fig. 18a the positive elastic moment augmented by the previous positive residual moment at the now critical hinge 4 would result in a value for beyond the available full plastic moment of the section. Hence plastic rotation of hinge 4 took place. The observed moments are also shown in Fig. 18a. Due to the rotation of plastic hinge 4 the residual moments are now

negative (Fig. 18b). Going from step (b) to step (c) (Figs. 19a and 19b) causes only unloading of all parts of the structure. No plastic deformation takes place and theoretically the residual moments remain unchanged. Actually the residual moments at the center support decreased from −19.8 in-kips to −21.4 in-kips. During step (a) of the next cycle the residual moments will become positive again and the same sequence will be repeated. Consequently, the deformations will increase during each cycle. When the residual moments are such that the sum of residual and elastic moments does not exceed M_2 and M_3 at Sections 2 and 3 respectively, the deflections will stabilize at the corresponding value δ_s.

IV. D I S C U S S I O N

The beams loaded proportionally were definitely stronger than predicted by the simple plastic theory that neglects strain-hardening. The maximum load applied (20 kips) was about 20% greater than predicted by theory. Had the test assembly permitted, the beams would have carried more load. Because of point loading and the elimination of buckling no convenient "leveling off" point was observed.

A deflection-rate criterion, selected in order to compare predicted with observed values, appears to be a reasonable method of comparing the results of proportional and cyclic loading tests. It is consistent with the real philosophy of plastic analysis, (the onset of deflections much greater than

those experienced at lower loads).

In the case of proportional loading this criterion leads to good agreement with theoretical predictions (Obs./Theor. 102 and 105%). However, in the case of cyclic loading the theory seems to underestimate the stabilizing load (Obs./Theor 108%).

It should be kept in mind that the deflection-rate criterion specified the lower limit of ultimate and stabilizing load. The test results show a correlation between the load deflection curve for proportional loading and the upper limit load vs. stabilized deflection curve for cyclic loading.

Beams with considerable length under near-uniform moment do not reveal the strain-hardening effect shown in Fig. 16. For such cases, the deflection-rate criterion possibly represents a value that would not be exceeded. Tests to explore this would be desirable. Another important factor may be the influence of buckling.

The loading cycle was undoubtedly more severe than would be encountered in practice ($\zeta = 0.07$). The actual reduction in load capacity was 13%. The theory of "deflection stability" predicts an 18% reduction.

These tests, therefore, show that "Instability of Deflection" may not be as severe a limitation to the application of plastic analysis to design as the theory would indicate. It need only be of concern when the important loads on a structure are subject to nearly complete fluctuation.

V. SUMMARY (TABLE 3)

1. Using the deflection-rate criterion, experimental values of the ultimate load, P_u were obtained which are in good agreement with theoretical predictions $\left(\frac{\text{Obs. value}}{\text{Theor. value}} = 102 \text{ to } 105\%\right)$

2. Due to point loading and strain-hardening loads increased beyond the computed ultimate load. A true "ultimate" load could not be obtained within the limits of the test set-up.

3. For the tested structure the theory underestimated the stabilizing load $\left(\frac{\text{Obs. value}}{\text{Theor. value}} = 109\%\right)$

4. However, the actual difference between stabilizing and collapse load of 13% is still considerable. It should be taken into account whenever complete load removal takes place.

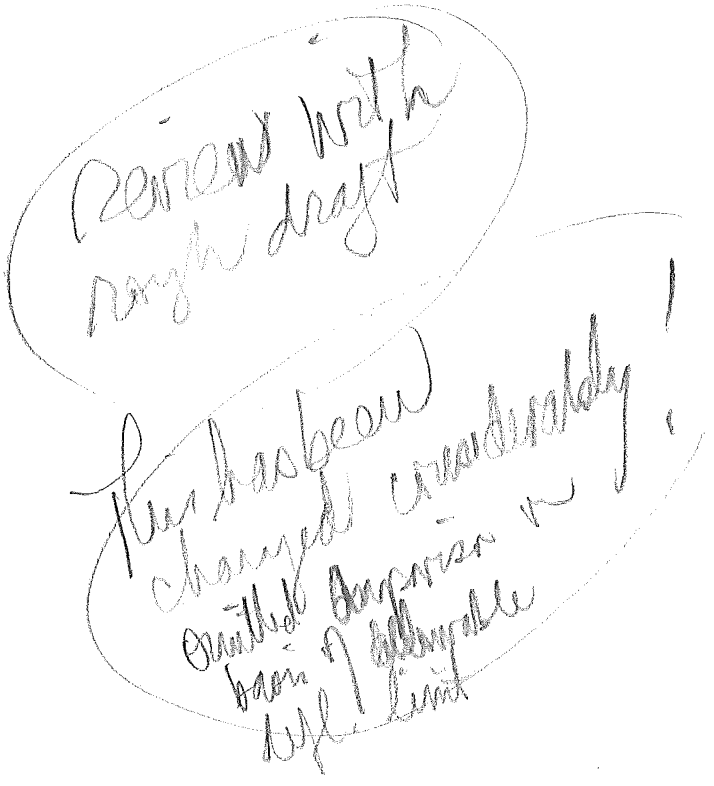

VI. REFERENCES

1. P.S. Symonds, "The Basic Theorems in the Plastic Theory of Structures", Journal of the Aeronautical Sciences, Vol. 17 No. 18, pp. 669-670, October, 1950.

2. C. Massonnet, "Essais d'adaptation et de Stabilization Plastiques sur des Poutrelles Laminees" Memoires, Association Internationale des Ponts et Charpentes, Vol. 13, pp. 239-282. 1953.

3. B.G. Neal, "Plastic Collapse and Shakedown Theorems for Structures of Strain-Hardening Materials", Journal of Aeronautical Sciences, Vol. 17 No. 5, pp. 297-306, May, 1950.

4. B.G. Neal, "The Behavior of Continuous Beams and Plane Frames Under Repeated Loading", Technical Report No. A11-32, Brown University to Office of Naval Research, April, 1949.

5. B.G. Neal and P.S. Symonds, "The Rapid Calculation of the Plastic Collapse Load for a Framed Structure", Structural Paper No. 29, Institution of Civil Engineers, London, 1952.

6. C.H. Yang, K.E. Knudsen, B.G. Johnston and L.S. Beedle, "Plastic Strength and Deflection of Continuous Beams" With an Appendix by W.H. Weiskopf, Progress Report No. 9 (205B.22), Fritz Laboratory, Lehigh University, November 24, 1952.

7. A.T. Gozum, "On Coupon Tests", Project Report No. 220A.13, Fritz Laboratory, Lehigh University, August, 1954.

8. J.W. Roderick and I.H. Phillips, "Carrying Capacity of Simply Supported Mild Steel Beams", Colston Papers, Vol. II, pp. 9 to 48, December, 1949.

VII. ACKNOWLEDGMENTS

This investigation has been carried out by the first author in fulfillment of the requirements of Course C.E. 404 "Structural Research" under the direction of Dr. Bruno Thürlimann to whom he wishes to express his sincere appreciation for supervision and guidance. The coauthor extended the theoretical considerations by showing the influence of strain-hardening.

The authors wish to express their appreciation to the entire Fritz Laboratory staff and personnel for their encouragement and great help.

This work has been carried out with funds furnished for shop services by the Institute of Research and the Department of Civil Engineering and Mechanics at Lehigh University. Materials were made available through the research program "Welded Continuous Frames and Their Components", carried out at Fritz Engineering Laboratory under the general direction of Dr. Lynn S. Beedle; the investigation is sponsored by: American Institute of Steel Construction, American Iron and Steel Institute, Column Research Council (Advisory), Navy Department (Contract 39303), Office of Naval Research, Bureau of Ships, Bureau of Yards and Docks, and Welding Research Council.

Table 1

Test Program - 4 WF13 Shape

Test No.	Loading Type	Loads	Remarks
P-1	Proportional	Two equal loads	See Fig. 1
P-2	Proportional	Single load	See Fig. 2
C-1	Cyclic*	P_L = 17.0^k	
C-2	Cyclic*	P_L = 14.75^k; 15.0^k; 15.25^k; 16.0^k.	
C-3	Cyclic*	P_L = 14.0^k; 15.5^k	

* Loading Cycle:

Step (a)

Step (b)

Step (c)

Step (d)

Step (e) = Step (a)

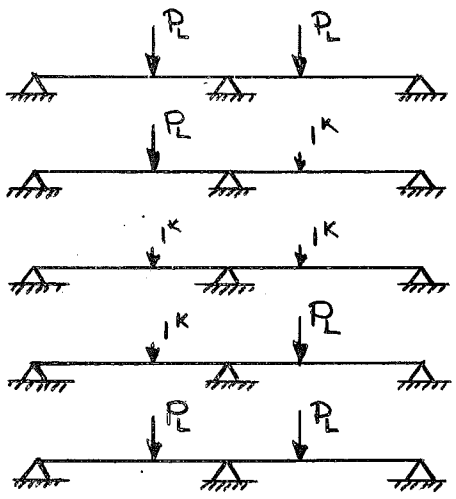

Table 2

Flange Tension Coupons

Yield Stress:

T-1 : σ_y = 39.30 ksi

T-2 : σ_y = 38.65 ksi

T-3 : σ_y = 37.40 ksi

T-4 : σ_y = 38.80 ksi

Material Properties:

Modulus of elasticity (assumed)	$E = 29.6 \times 10^3$ ksi
Yield Stress (average of coupons)	$\sigma_y = 38.5$ ksi

Geometrical Properties:

Flange width	$b = 4.117$ in.
Flange thickness (tapering) average	$t = 0.366$ in.
Depth	$d = 3.808$ in.
Web thickness	$w = 0.2906$ in.
Section modulus (weak axis)	$S = 2.073$ in.^{3}
Plastic modulus (weak axis)	$Z = 3.143$ in.^{3}
Moment of inertia (weak axis)	$I = 4.269$ in.^{4}
Shape factor	$f = 1.516$

Section Properties of Shape:

Yield moment	$M_y = 79.83$ in. kips
Plastic moment	$M_p = 121.0$ in. kips
Curvature at initial yield	$\phi_y = M_y/EI = 0.63 \times 10^{-3}$ rad./in
Available elastic moment range	$\Delta M_y = 2M_y = 159.6$ in. kips

Table 3

Summary of Test Results

(a) Proportional Loading, P_u (kips)

Test	Theoretical Simple Pl. Theory	Observed					
		Equalization of moments		Defl. Crit. Massonnet(2)		Defl. Rate Criterion	
			Obs./Theor.		Obs./Theor.		Obs./Theor.
P-1 (case a)	16.81	16.00	95.2%	17.58	104.6%	17.08	101.6%
P-2 (case b)	16.81	18.00	107.1%	17.78	105.8%	17.68	105.2%

(b) Proportional and Cyclic Loading, P_u and P_s

	P_u kips	P_s kips	P_s/P_p
Simple Plastic Theory	16.81	13.7	81.6%
Observed (deflection-rate criterion)	17.08 $\frac{\text{Obs.}}{\text{Theor.}}$ = 101.6%	14.80 $\frac{\text{Obs.}}{\text{Theor.}}$ = 108%	86.8%

See 8P Flowchart

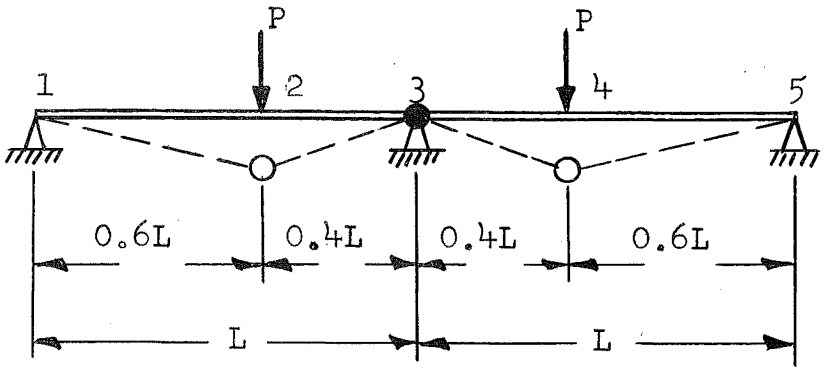

FIG. 1 CASE (a) - PROPORTIONAL LOADING WITH TWO LOADS

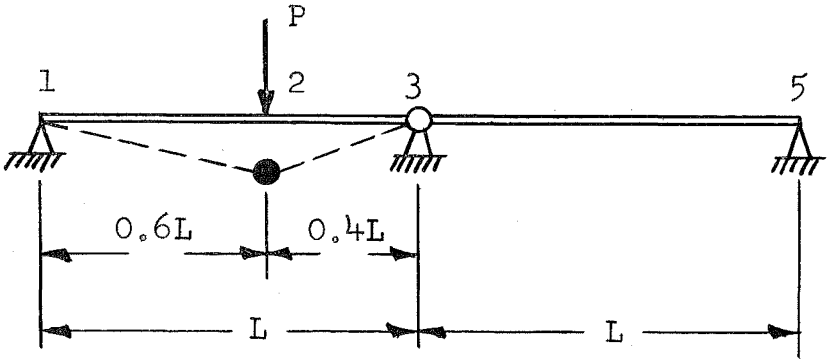

FIG. 2 CASE (b) - PROPORTIONAL LOADING WITH ONE LOAD

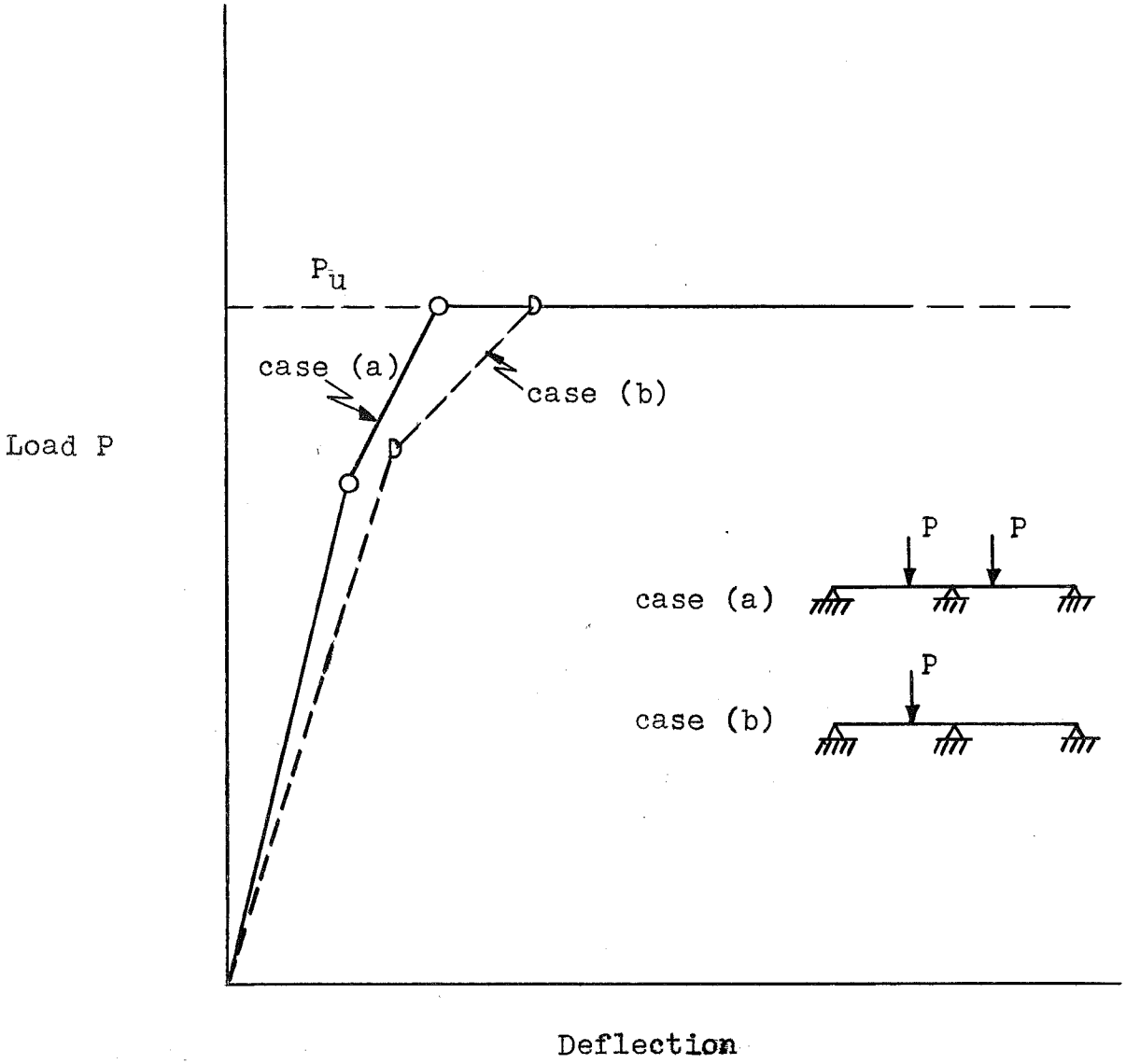

FIG. 3 SIMPLIFIED DEFLECTION LOAD VS. DEFLECTION CURVES

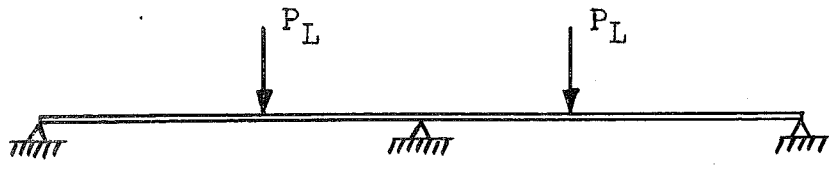

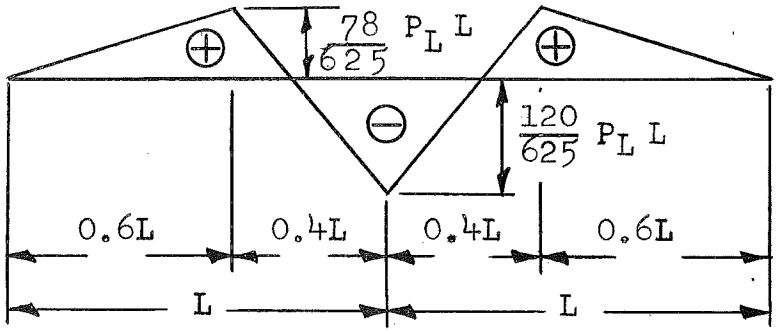

FIG. 4a

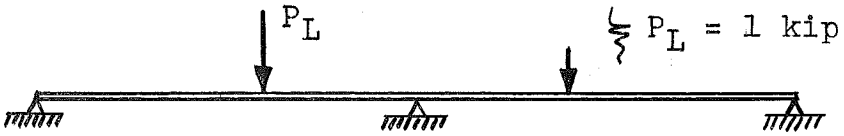

FIG. 4b

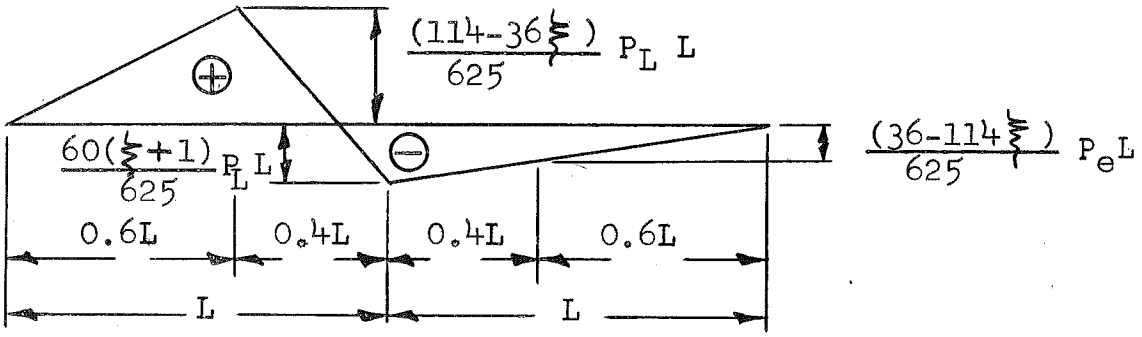

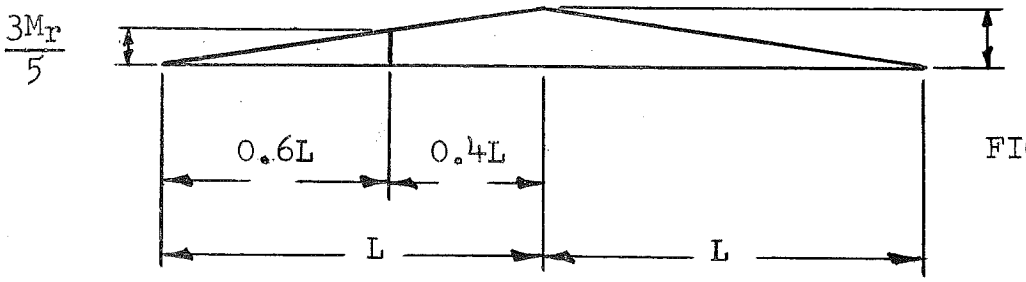

FIG. 4c

FIG. 4 MOMENT DIAGRAMS FOR CYCLIC LOADING

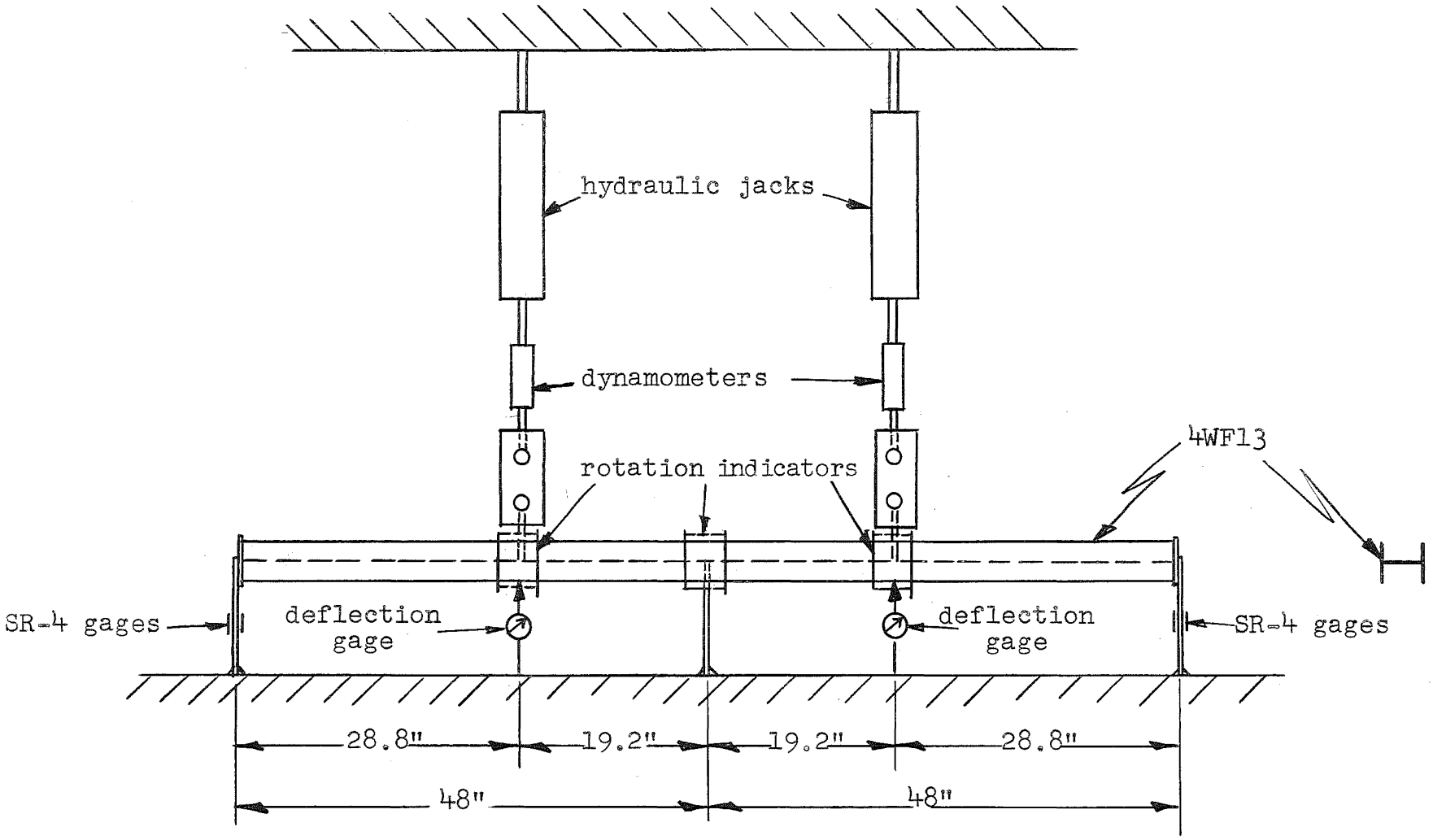

FIG. 5 TEST SET-UP

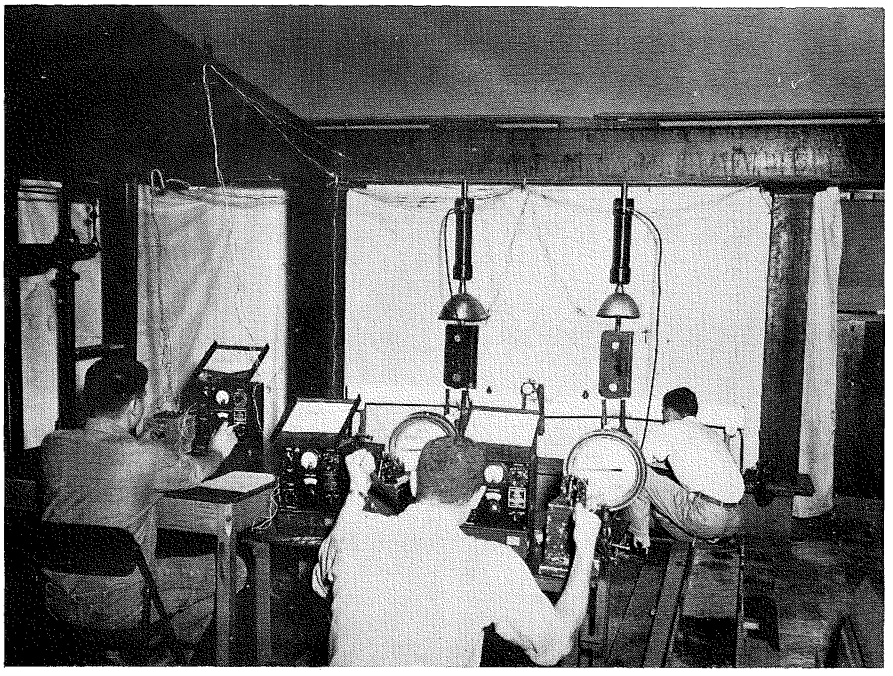

FIG. 6 GENERAL VIEW OF TEST SET-UP

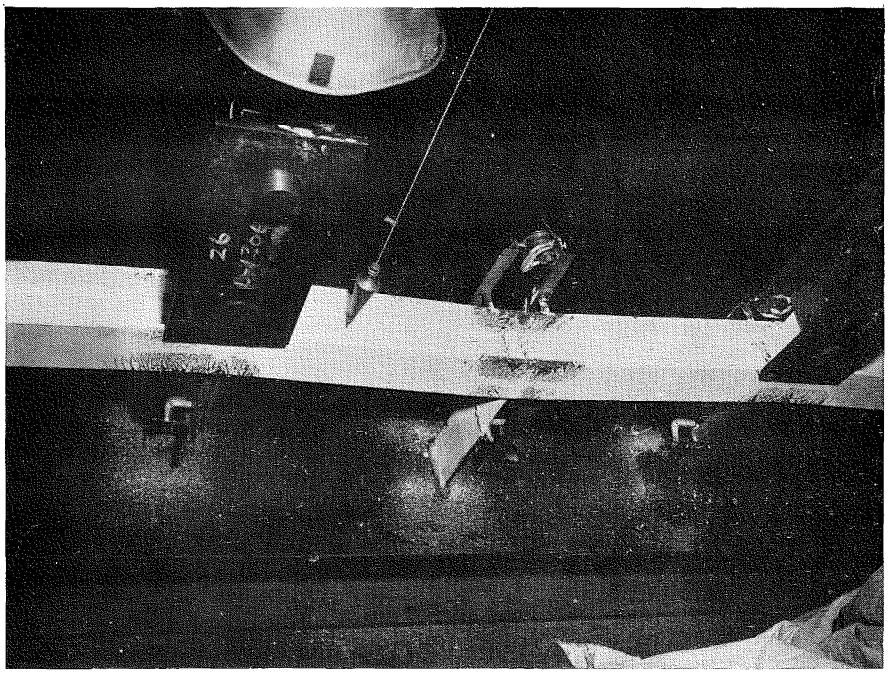

FIG. 7 EXTENT OF YIELD AT THE PLASTIC HINGES

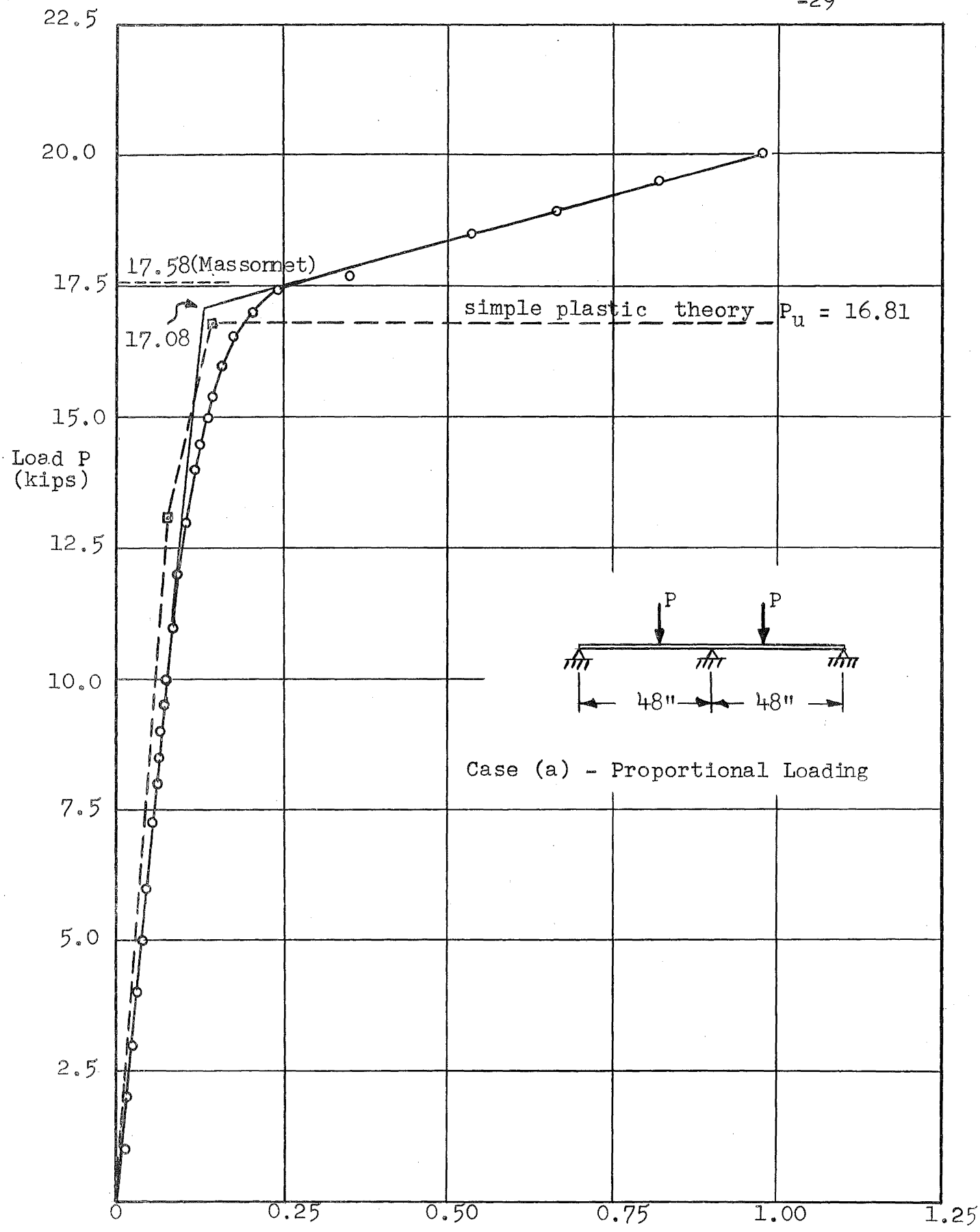

FIG. 8 LOAD VS. DEFLECTION CURVE FOR TEST P-1

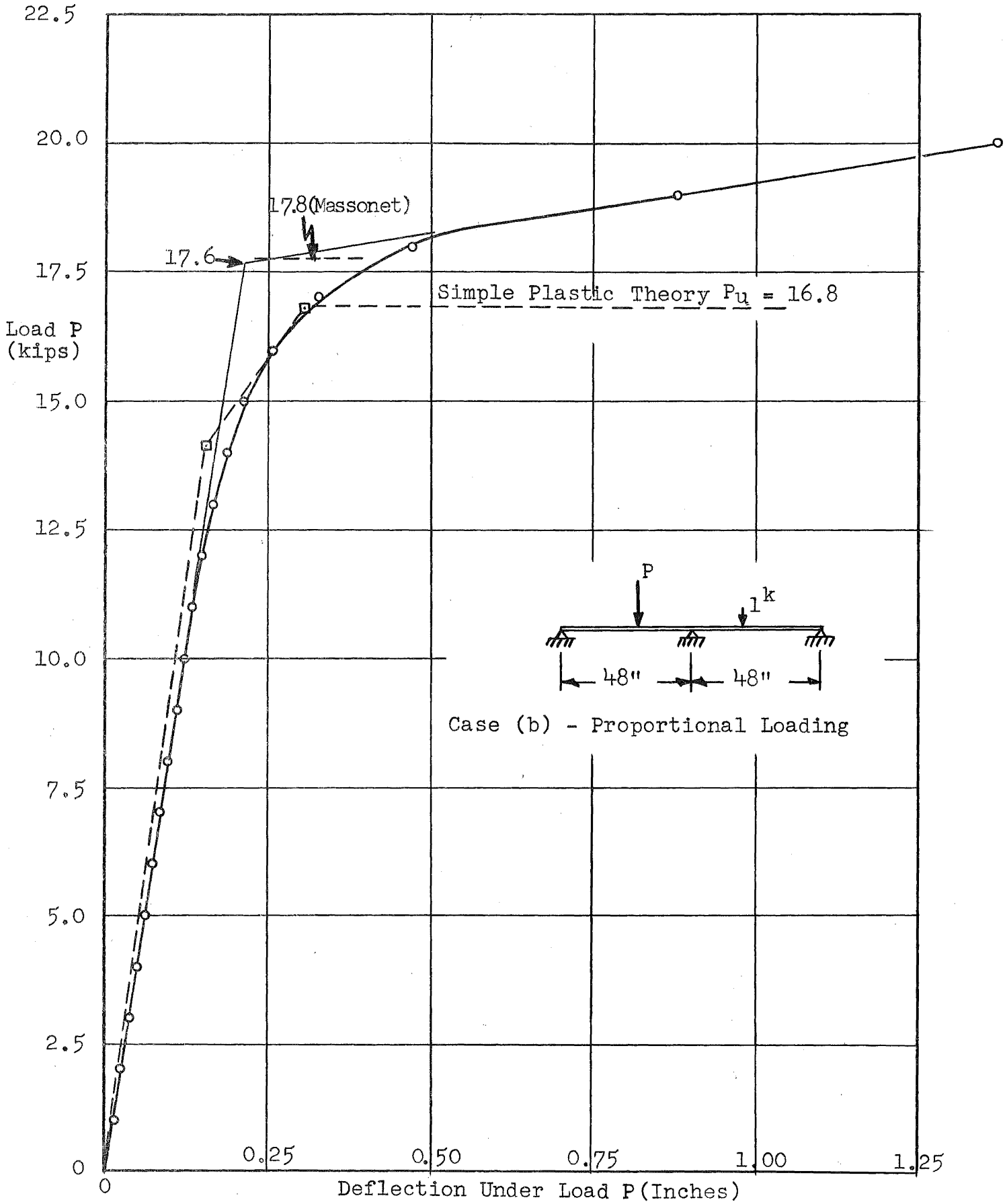

FIG. 9 LOAD DEFLECTION CURVE FOR TEST P-2

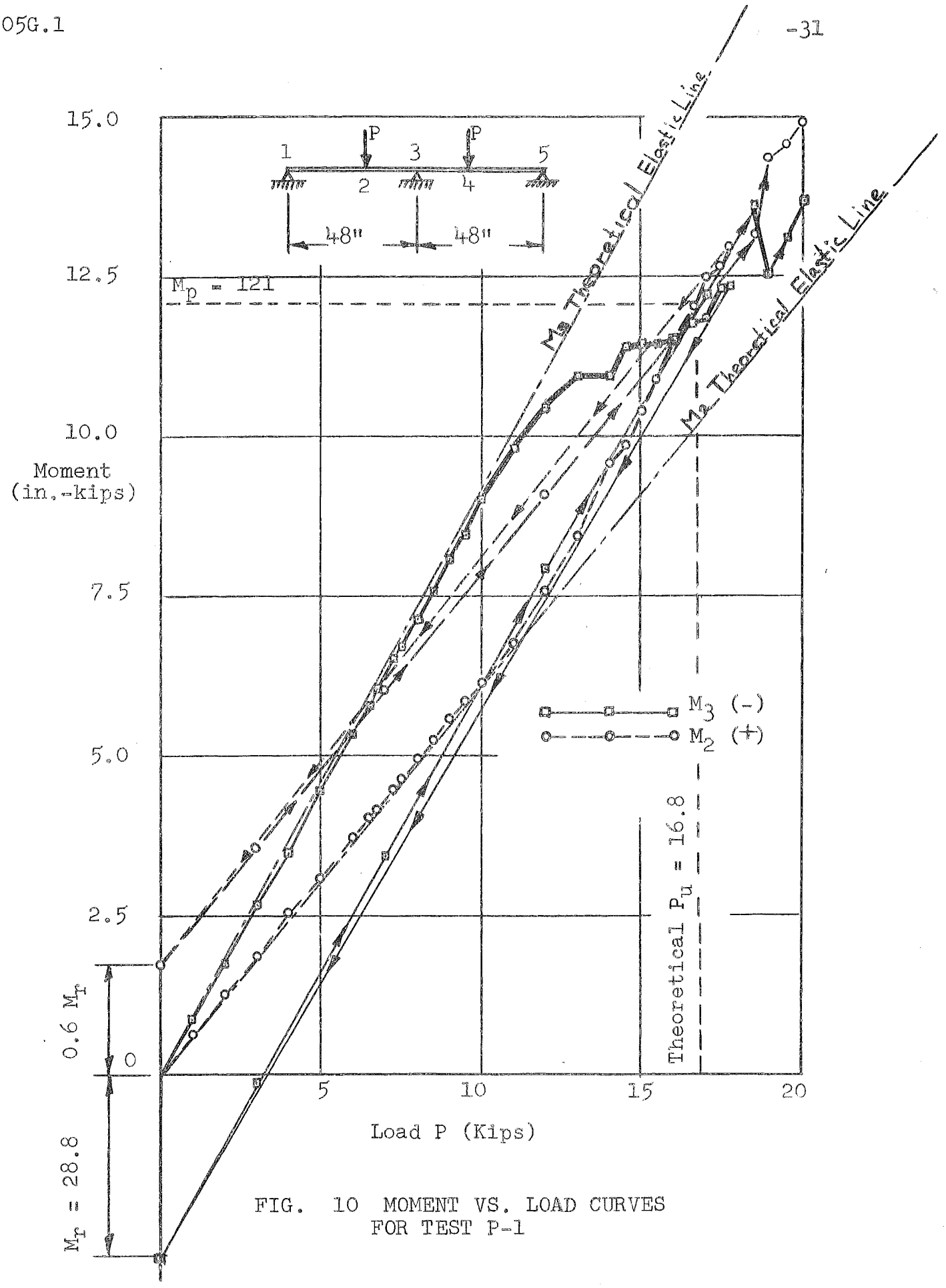

FIG. 10 MOMENT VS. LOAD CURVES FOR TEST P-1

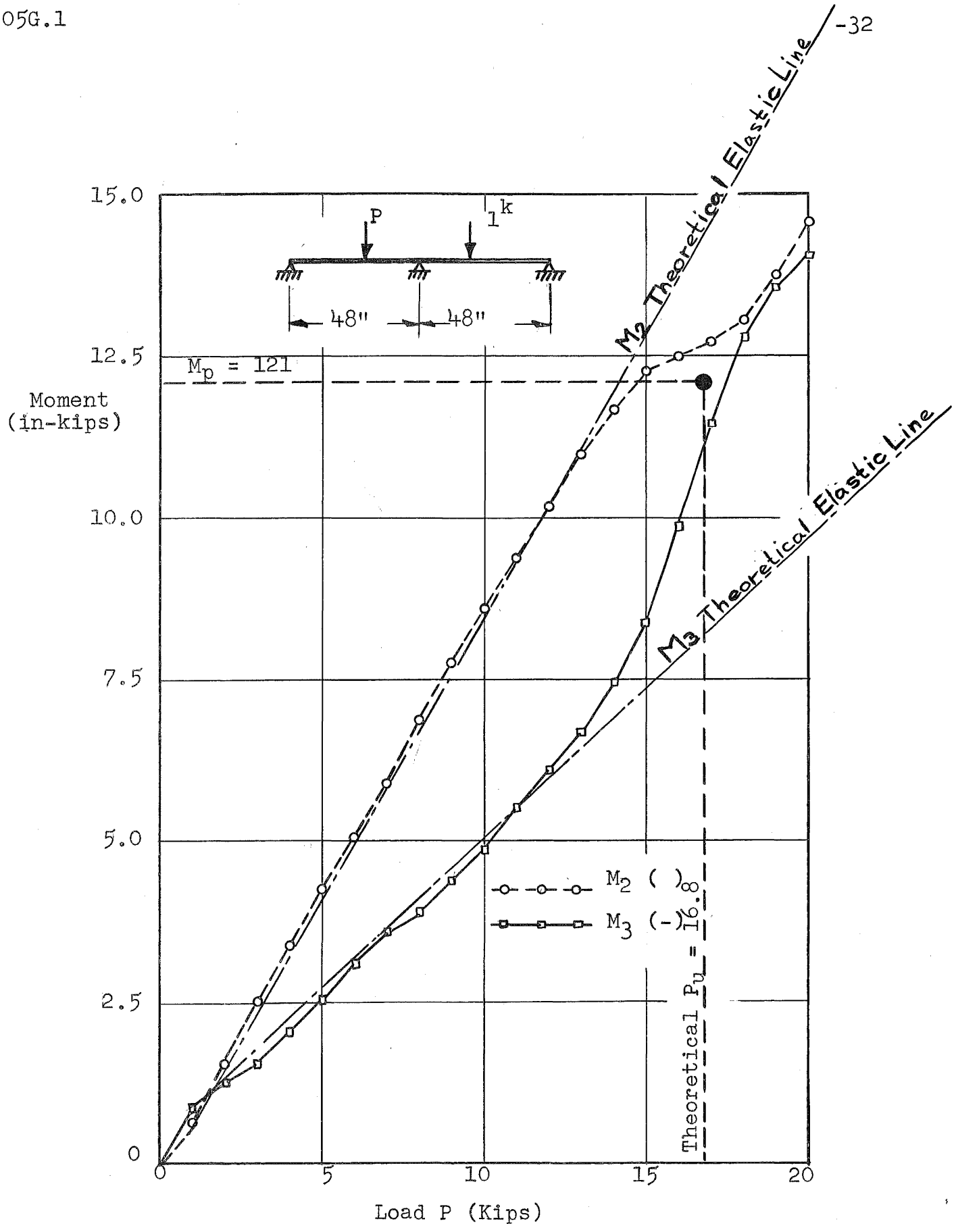

FIG. 11 MOMENT VS. LOAD CURVES FOR TEST P-2

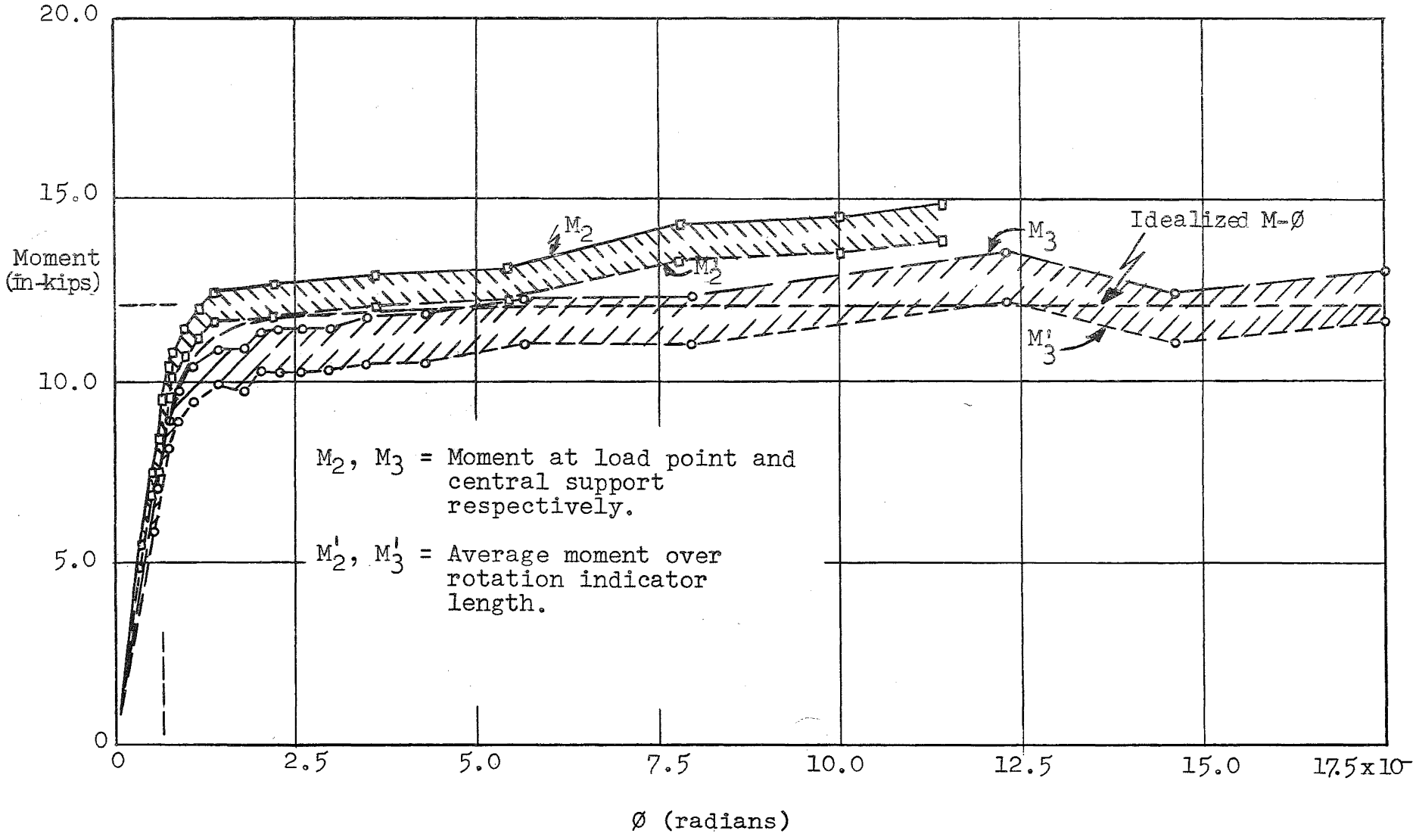

FIG. 12 M-Ø CURVES FOR TEST P-1

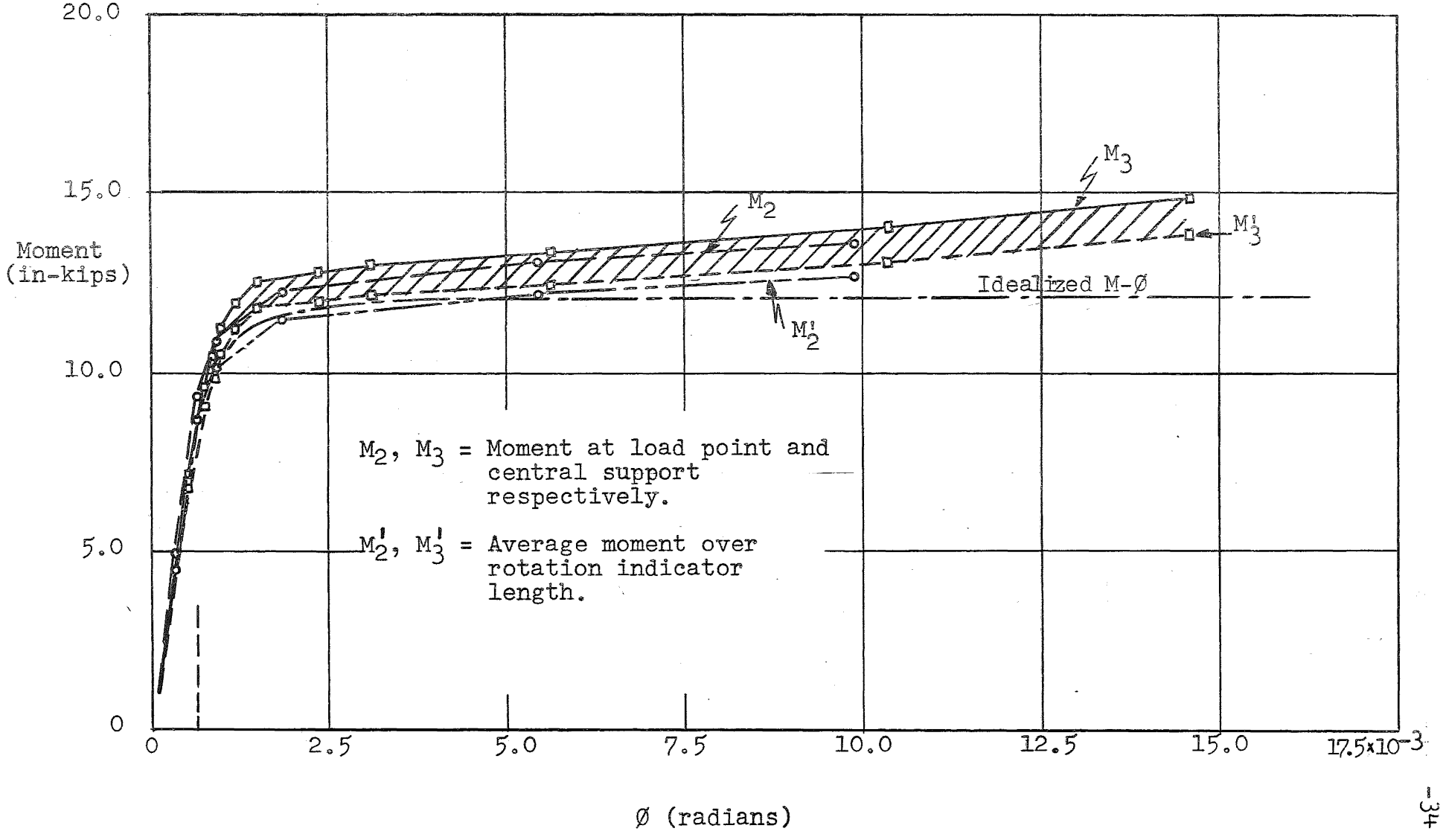

FIG. 13 M-Ø CURVES FOR TEST P-2

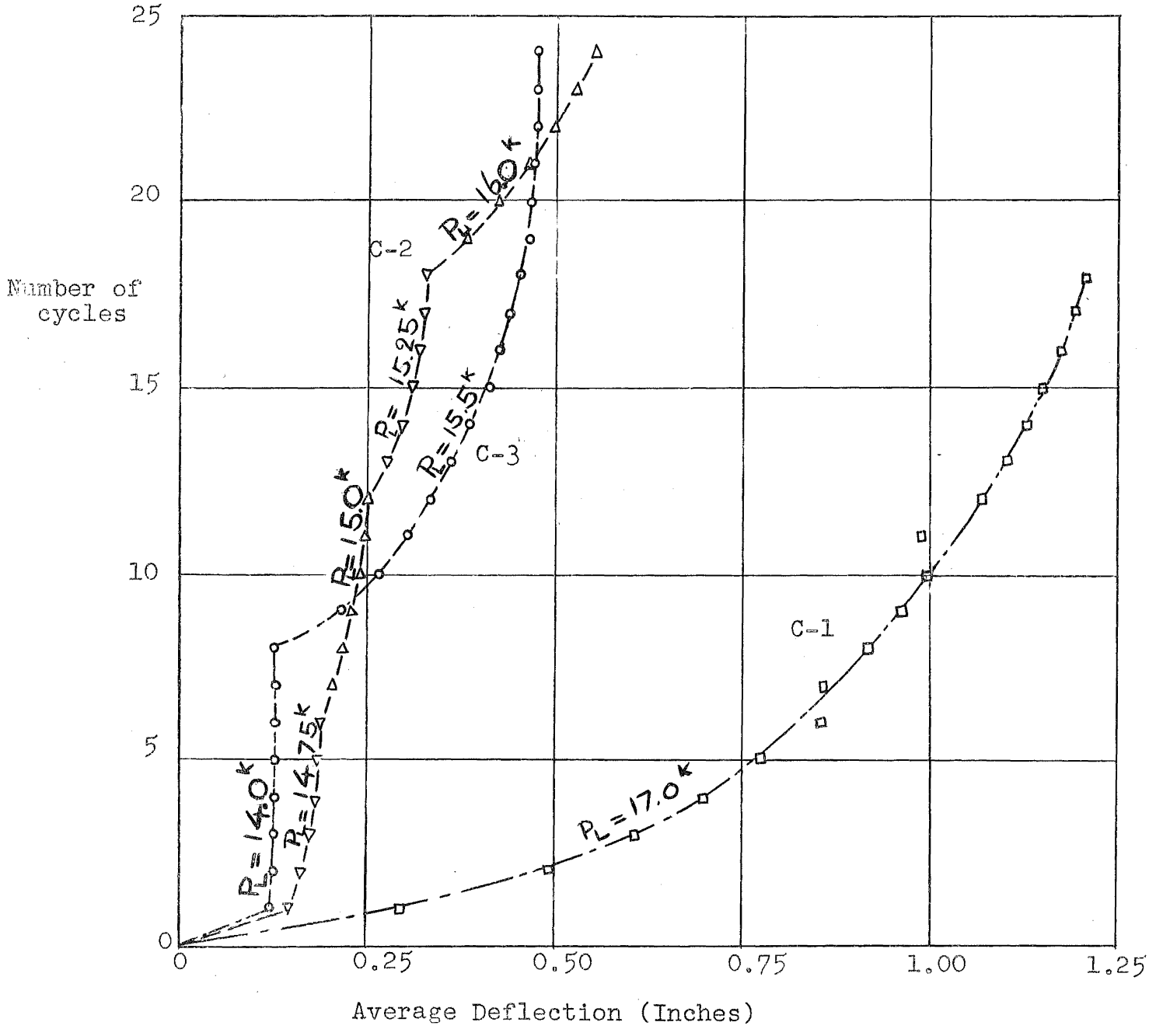

FIG. 14 RESULTS OF CYCLIC LOADING TESTS

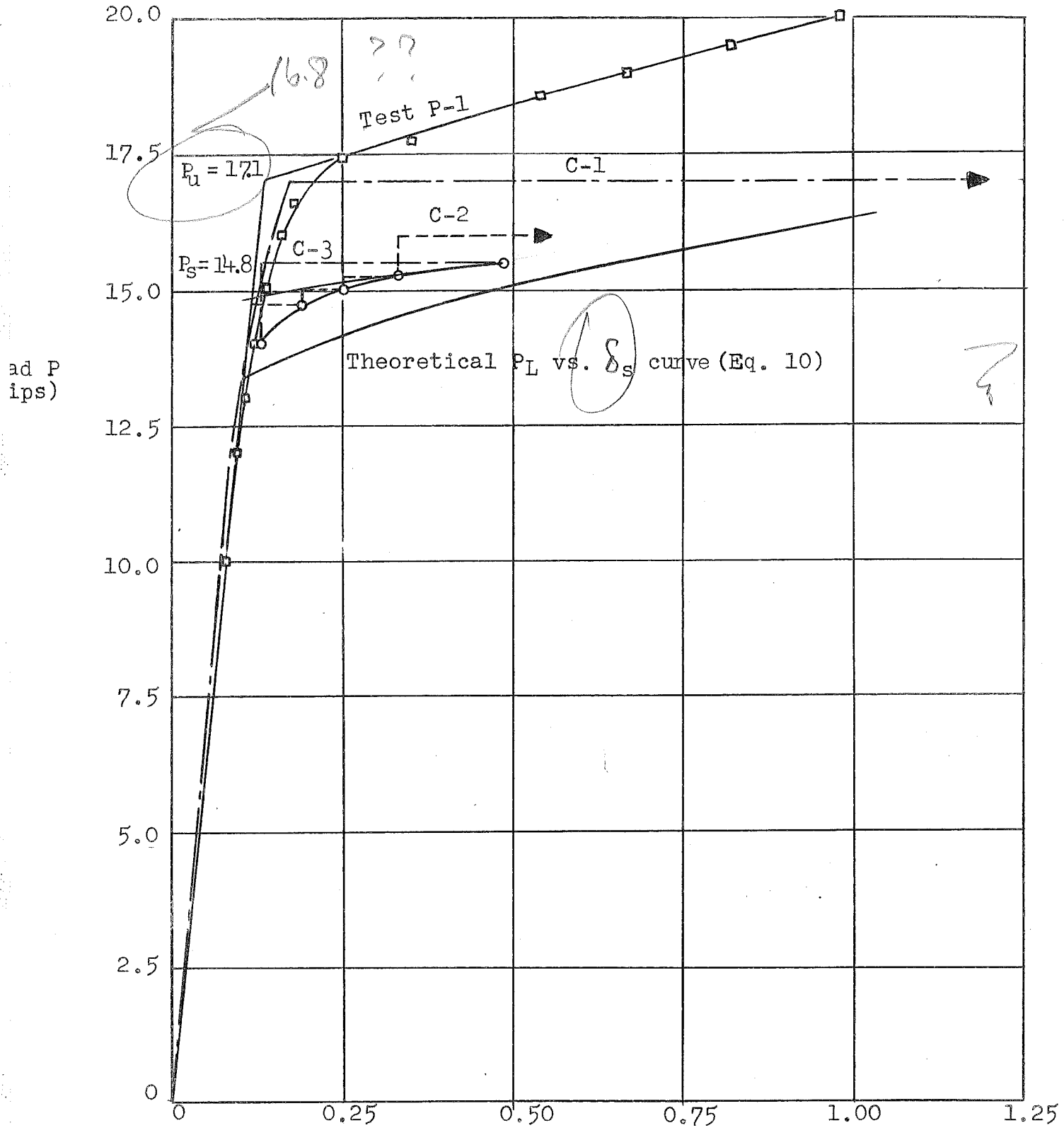

FIG. 15 RESULTS OF PROPORTIONAL AND CYCLIC LOADING TESTS; P-1, AND C-1, C-2, C-3

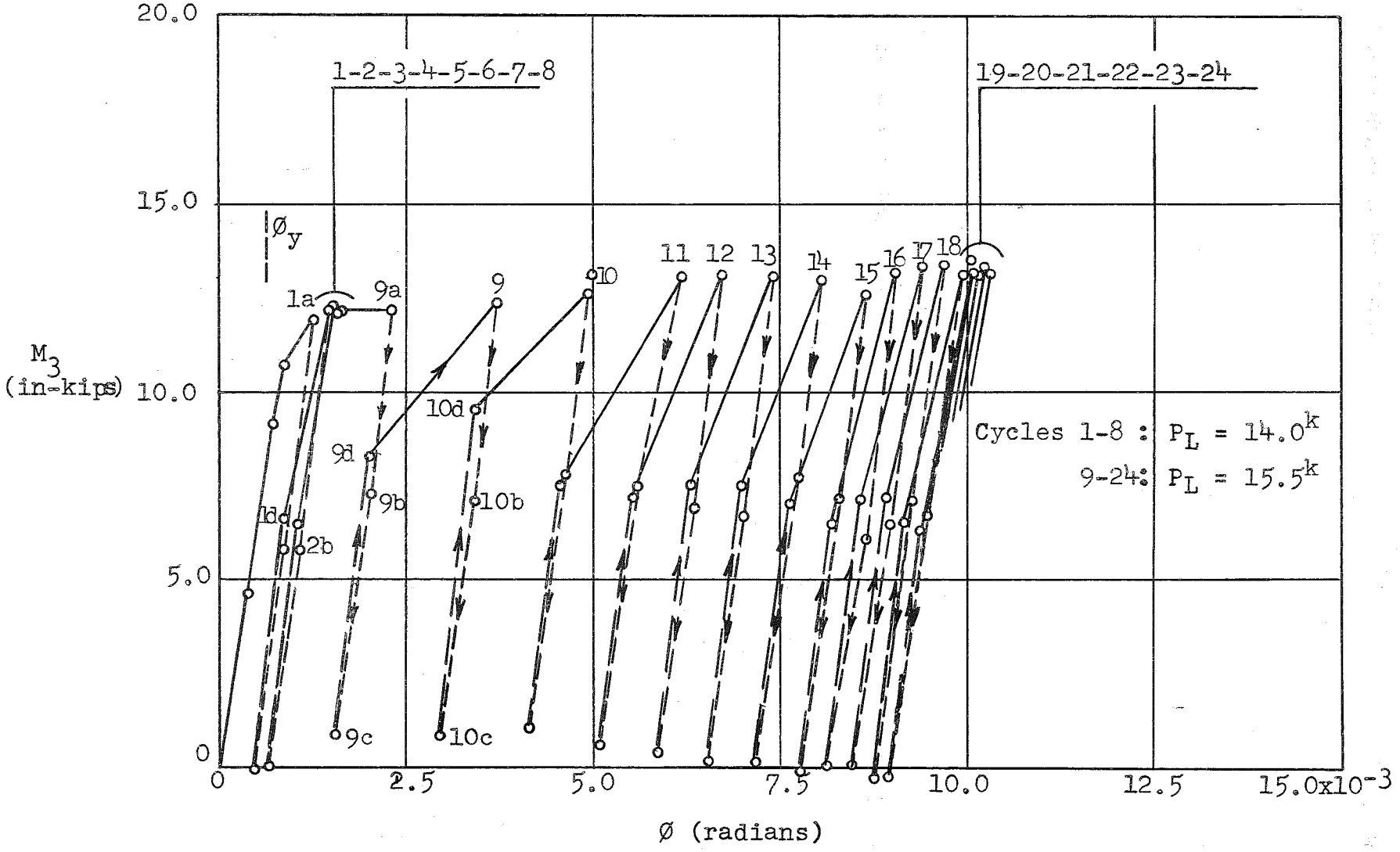

FIG. 16 M_3 VS. Ø FOR CYCLIC LOADING TEST C3

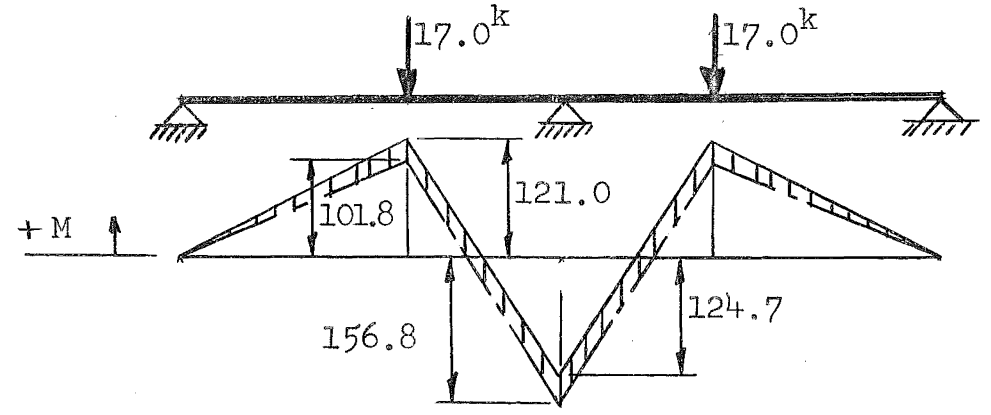

FIG. 17(a)

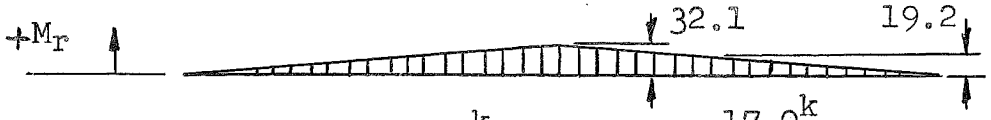

FIG. 17(b)

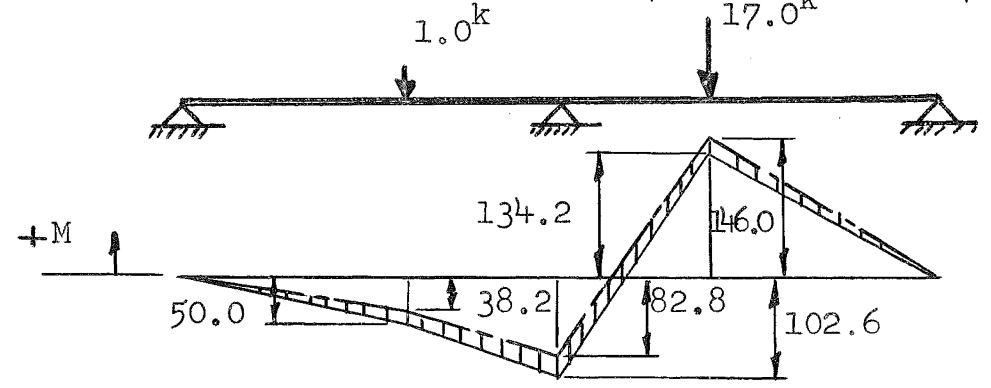

FIG. 18(a)

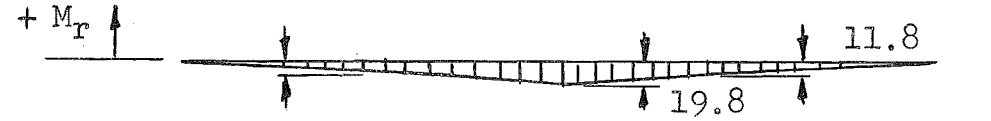

FIG. 18(b)

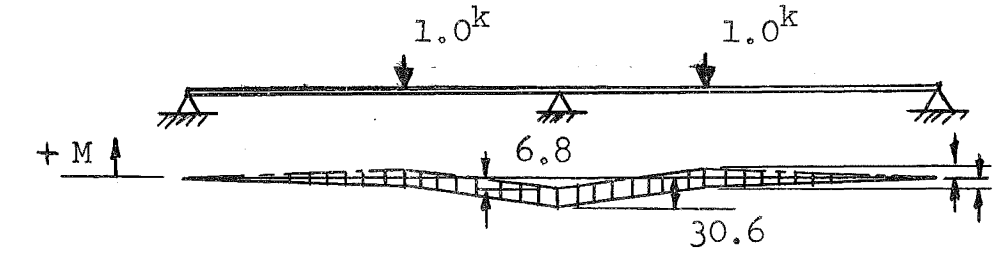

FIG. 19(a)

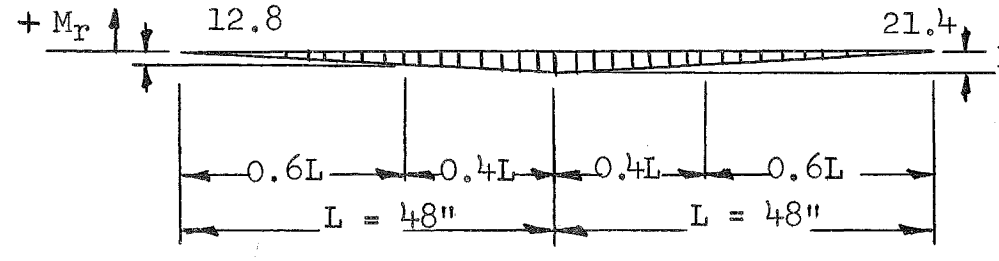

FIG. 19 (b)

——·——·—— Computed Elastic Moment (in-kips)

———————— Observed Moment (in-kips)